

## Empirical Force Field Calculations on Tetraarylmethanes and -silanes. II. Dynamic Stereochemistry

M. G. Hutchings, Joseph D. Andose, and Kurt Mislow\*

Contribution from the Department of Chemistry, Princeton University, Princeton, New Jersey 08540. Received October 22, 1974

**Abstract:** Empirical force field calculations of the isomerization pathway of tetraphenylmethane indicate a mechanism involving a sixfold energy potential for the isomerization (topomerization). The strain energy of the calculated transition state is 14.9 kcal/mol above the  $D_{2d}$  ground state, corresponding to the activation energy for the topomerization. An extensive series of similar calculations on tetra-*o*-tolylsilane (TTS) indicates that the same type of mechanism is operative, this mechanism being the least motion pathway. Repeated isomerization by this mechanism alone will result in the rapid equilibration of all conformers of TTS at ambient temperatures. With the aid of a permutational analysis, it is shown that a sequence of no fewer than four such isomerizations is required to effect topomerization of the ground state conformer of TTS, and consequently to explain earlier DNMR results on tri-*o*-tolyl-1-naphthylsilane. The calculated activation energy of less than 19.6 kcal/mol for the TTS topomerization compares with the upper limit of 16 kcal/mol estimated on the basis of the DNMR study. An additional lower energy rocking motion is responsible for equilibrating some conformers of TTS. It is concluded that residual diastereomerism will be absent in tetraarylmethanes if the least motion pathway is available for stereoisomerization.

In the preceding paper<sup>1</sup> (hereafter referred to as part I) we presented results of an investigation into the static stereochemistry of tetraarylmethanes and -silanes by a full relaxation empirical force field approach. In this paper, we continue our discussion of the stereochemical features of these species, focusing our attention on their dynamic behavior. The conventions we shall use herein are those introduced previously in part I.

Experimental studies of the conformational dynamics of tetraarylmethanes and cognates are sparse. Our own DNMR studies<sup>2</sup> of tetra-*o*-tolylsilane (TTS) and related molecules yielded a barrier for isomerization in TTS of less than 16 kcal/mol, by extrapolation from the 13.5 kcal/mol measured for tri-*o*-tolyl-1-naphthylsilane (TNS). On the basis of these results, it was concluded that the previously reported<sup>3</sup> isolation of stable conformers of TTS must be in error. Subsequently, we went on to suggest an intuitive mechanism for the isomerization.<sup>4</sup> The question of corroborative evidence for this mechanism remained, however. Apart from our study, the only other tetraarylmethane cognates to have been investigated were tetrakis(pentafluorophenyl)germane and related molecules.<sup>5</sup> Line broadening effects in the <sup>19</sup>F NMR spectra of some of these species were suggested to be due to hindered rotation.<sup>5</sup> However, variable temperature measurements<sup>5a</sup> fail to support this hypothesis.

The investigation in part I of the tetra-*o*-tolylmethane (TTM) and TTS systems by empirical force field calculations revealed that in each case the energy minima corresponded to six diastereomeric conformers, comprising two achiral forms of  $S_4$  symmetry, and four chiral structures (one of  $C_2$  symmetry and the other three asymmetric); cf. Figure 5, part I.<sup>6</sup> All are based on a skeleton of  $S_4$  or  $\psi$ - $S_4$  symmetry. Each of the conformers with an endo (*n*) substituent can be derived from the (*xxxx*) conformer, at least in a formal sense, by flipping one or a combination of the *o*-tolyl groups through  $\pi$  radians.

In a brief discussion of the stereochemistry of TTS, Cahn, Ingold, and Prelog made the persuasive suggestion that the rotational barrier for each *o*-tolyl group is threefold in nature, by analogy with the pentaerythritol tetrahalides.<sup>7</sup> It was argued that each *o*-tolyl group can assume three space relations with the remaining tri-*o*-tolylsilane moiety (Figure 1). If each *o*-tolyl were constrained in any one of these three orientations relative to the other three

groups, nine isomers would be possible (three meso compounds and three *dl* pairs, i.e., (*xxxx*) and 1–5, Figure 2). However, this description does not accord with the conclusions arrived at on the basis of strain minimization calculations (part I): only one conformer is stable, (*xxxx*), and the others (1–5, Figure 2) relax to one of five diastereomeric conformers with  $S_4$  or  $\psi$ - $S_4$  symmetry (cf. Figure 5 and Table II, each in part I).

How do we account for the failure of the ostensibly reasonable model on which Cahn, Ingold, and Prelog based their analysis? The answer lies in the concept of *correlated rotation*.<sup>8</sup>

The notion of a threefold barrier is well-grounded only if the torsional motion of the rotor is assumed to be independent of the other groups present in the molecule, so that the

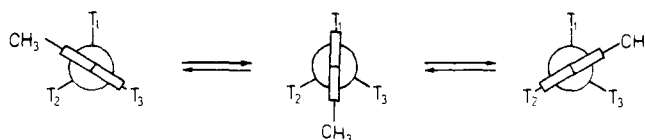


**Figure 1.** Newman projections of the three orientations adopted by an *o*-tolyl group with respect to the remaining tri-*o*-tolylsilane moiety in tetra-*o*-tolylsilane, according to ref 7.

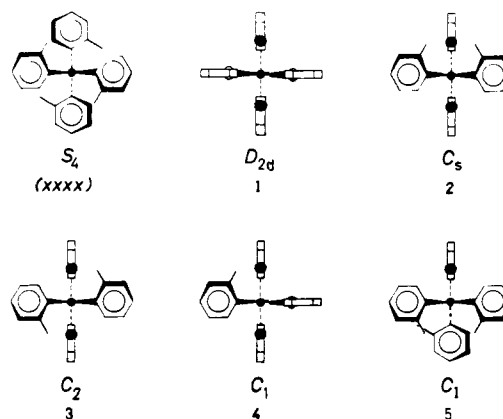


**Figure 2.** The six diastereomeric conformations of tetra-*o*-tolylsilane based on the threefold torsional potential suggested in ref 7.

only energy barrier to overcome is the eclipsing (Pitzer) strain, as was assumed to be the case for the pentaerythritol tetrahalides.<sup>7,9</sup> However, the *o*-tolyl groups of TTM and TTS are sufficiently bulky so as to render independent torsions unrealistic, and the description of the system therefore becomes more complex than previously envisaged. In other words, the perturbation of one aryl group, which we shall call the reference ring, from its equilibrium position necessarily induces sympathetic motions of the other groups which will tend to compensate for any increased steric strain; i.e., the rotations are correlated. As a result of these composite motions, a new equilibrium conformation may be attained earlier in the rotation of the reference ring than otherwise expected, by virtue of the other three rings themselves adopting a new arrangement which allows of overall  $S_4$  or  $\psi$ - $S_4$  symmetry. This situation requires a new pairing of aryl rings, and a simultaneous reorientation of the  $S_4$  or  $\psi$ - $S_4$  axis. Since the reference ring can be paired with any of the three other rings, in both endo and exo orientations, there are a total of six positions which the aryl group may adopt during a full cycle of  $2\pi$  radians in each of which the whole molecule will be of  $S_4$  or  $\psi$ - $S_4$  symmetry.

In the remainder of this paper we shall discuss results of the determinations of the transition states for stereoisomerization of tetraarylmethane derivatives by the empirical force field approach, with a view to determining the mechanisms and energetics of these processes. The results thus obtained will serve to illustrate and clarify the implications of the concepts we have just introduced.

## Results and Discussion

Two systems were chosen for detailed study, using the incremental ring driving technique, outlined in an earlier paper,<sup>10</sup> which involves method II described in Part I. Tetraphenylmethane (TPM), the parent compound of the methane series, was considered desirable for this study because of its highly symmetrical ground state and substitution pattern, and because there are no data available on the barriers to isomerization of any tetraarylmethane derivatives. It was hoped that this study would indicate the magnitude of the barriers to be expected in such compounds, as well as the mechanism of isomerization. The other system is TTS. The experimental study of TTS and closely related species<sup>2</sup> provides a yardstick in this case with which the results of such calculations might be compared; furthermore, it was clearly desirable to furnish corroboration or otherwise for our previously postulated mechanism of isomerization of TTS.<sup>4</sup>

**Tetraphenylmethane.** The input structure used for this study was of  $^{\circ}D_{2d}$  symmetry, with parameters as reported in part I. Because of the high symmetry of this arrangement, there is only one possible manner in which to drive one ring. Initial increments of  $15^\circ$  were followed by increments of  $10$ ,  $7.5$ , and  $2.5^\circ$  as the transition state was approached. The relative strain energies as a function of the angle through which a phenyl ring was driven are recorded in Table I.

The overall mechanism is depicted diagrammatically in Figure 3. Starting with the  $^{\circ}D_{2d}$  conformation, as ring 1 is driven in a clockwise direction (viewed toward the center of the molecule), the other three rings rotate into an approximate  $S_4$  conformation, but at all times remain in a more open orientation than the driven ring. As the transition state is approached, rings 2 and 3 begin to reverse their direction of rotation. The transition state is reached when the driven ring has been rotated  $96^\circ$ , that is, just past the closed orientation. An ORTEP stereopair of the transition state is reproduced in Figure 4. Further ring driving opens the possi-

Table I. Strain Energy of Tetraphenylmethane as a Function of the Angle of the Driven Ring

$E_T^b$	$\phi^a$			
	1	2	3	4
15.9 <sup>c</sup>	88.8	88.5	-88.8	-89.2
16.8	73.6	81.6	-79.8	-79.1
19.1	58.6	74.3	-69.8	-69.9
22.2	43.6	68.9	-61.9	-61.4
24.4	33.6	66.1	-57.2	-56.9
26.4	23.6	64.4	-53.6	-51.8
28.3	13.6	64.9	-51.9	-48.7
29.8	3.6	67.6	-53.4	-46.1
30.6	-3.9	71.1	-58.3	-43.3
30.8 <sup>d</sup>	-6.4	70.8	-59.1	-42.4
30.7	-8.9	73.0	-63.6	-40.7
27.0	-16.4	79.5	88.7	-28.8

<sup>a</sup> Indexing of rings follows Figure 3. Ring 1 is the driven ring. Angles are in degrees. <sup>b</sup> In kcal/mol. <sup>c</sup> Ground state. <sup>d</sup> Taken to be the transition state.

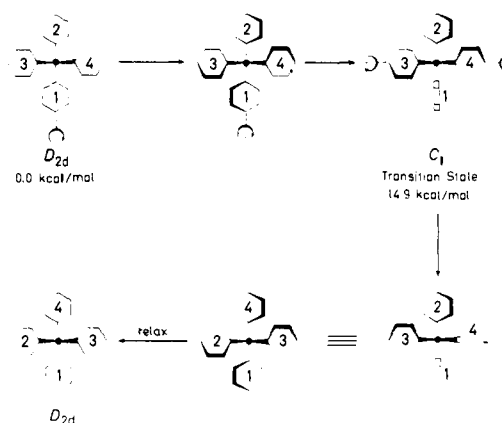


Figure 3. The mechanism of isomerization of tetraphenylmethane as determined by empirical force field calculations. The ring indexed 1 was driven in increments and all other groups allowed free relaxation.

bility for ring 3 to rotate past the obstruction originally caused by the *o*-hydrogen of ring 1 (arrow, Figure 3). Synchronously, ring 4 rotates markedly to a less open orientation (arrow, Figure 3). If the molecule at this juncture is reoriented so as to be viewed down a molecular axis bisecting the angle defined at the central carbon by the two bonds to aryl groups 2 and 3, it is seen that a new conformation of approximately  $S_4$  symmetry has been generated (Figure 3). Removal of constraints at this stage and subsequent full relaxation of this structure gives TPM in the  $^{\circ}D_{2d}$  conformation, but with a different pairing of phenyl rings: isomerization (topomerization) has taken place.

To attain the transition state conformation, ring 1 is forced to rotate  $36^\circ$  further, i.e., by  $96^\circ$ , than required for its net overall rotation of  $60^\circ$ . In other words, once the transition state has been passed, ring 1 rotates back by  $36^\circ$ . Thus, the driven ring, which we can regard as the reference ring, has passed through one-sixth of a full rotation of  $2\pi$  radians, implying a sixfold potential for the preferred mechanism. Figure 5 portrays a potential energy diagram for repeated topomerizations, the presentation adopted emphasizing the sixfold nature of the process. The total strain energy of the system ( $E_T$ ) is represented as the magnitude of a radial vector and has been plotted on polar coordinates as a function of the angle of torsion,  $\alpha$ , of ring 1. The diagram should be scrutinized in a clockwise direction, starting with the structure which corresponds to the ground state labeled  $\Delta$ . Each of the formula sketches depicts a ground state

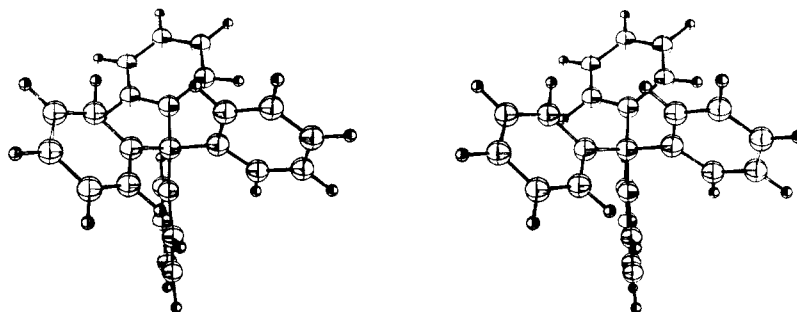


Figure 4. An ORTEP stereopair of the transition state for the isomerization of tetraphenylmethane, observed down the original  $S_4$  axis.

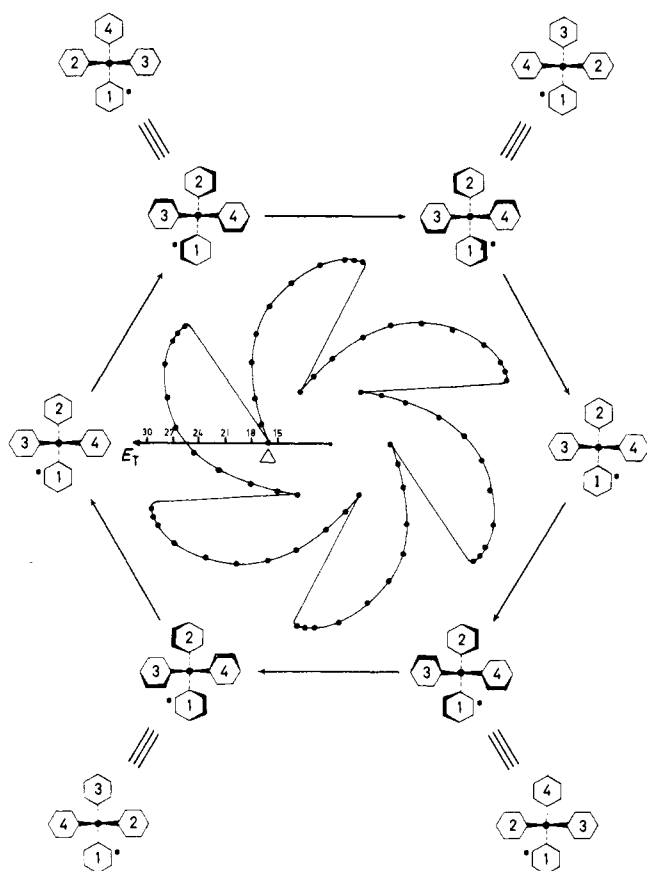


Figure 5. A potential energy diagram to emphasize the sixfold periodicity of the calculated mechanism of stereoisomerization in tetraphenylmethane, showing the driven ring (indexed 1) rotating through  $2\pi$  radians.  $E_T$  is in kcal/mol.

structure obtained during the full rotation of the driven ring. The outer one of the two sets of views clarifies the  $^{\circ}D_{2d}$  symmetry of the equilibrium structures, while the inner one shows each structure observed down a fixed molecular axis, thus easing perception of the fact that the driven ring is passing through  $2\pi$  radians. One of the ortho positions of the driven ring has been starred to clarify the point further.

The unsymmetrical appearance of the pinwheel plot in Figure 5 is due simply to the fact that we have considered thus far only the consequences of driving ring 1 in a clockwise direction. When ring 1 is driven in a counterclockwise direction, the same computations necessarily lead to a plot similar to that in Figure 5 but in which the direction of the outer arrows is now reversed and in which the pinwheel diagram now possesses the *opposite* two-dimensional chirality. Superposition of the right- and left-handed pinwheels

gives a beautifully symmetrical sixfold rosette ( $D_{6h}$ ), as required by microscopic reversibility.

We also wish to draw attention to an interesting dichotomy in pathways which is evident on inspection of Figure 5 and which may be stated as follows: each structure can be converted to two different topomers, depending on whether it *initially* follows the  $36^{\circ}$  route to the transition state, corresponding to the approximately straight line portion of the pinwheel blade (path A), or the  $96^{\circ}$  route, corresponding to the curved portion of the blade (path B). For example, starting with the "western" structure in Figure 5 (which is the starting structure in Figure 3), *driving* ring 1 in a clockwise direction as described above leads by path B to the "northwestern" structure in Figure 5 (which is the product of the sequence in Figure 3), whereas a  $36^{\circ}$  clockwise motion of ring 1 along the straight line itinerary, followed by a  $96^{\circ}$  counterclockwise motion after the transition state has been reached (path A), leads to the "southwestern" structure (see Figure 5). On the other hand, *driving* the same ring in a counterclockwise motion leads by path B on the mirror image pinwheel (not shown) to the southwestern structure, whereas path A leads to the northwestern structure. The question is: which of the two competing pathways (path A or B) to the transition state for each initial direction of motion (clockwise or counterclockwise) is preferred by the molecule? It appears to us that the answer must be neither. However, even though the transition state may be reached from either direction with equal probability, the program which underlies our computational method,<sup>10</sup> which involves ring driving, forces the molecule to follow that route in which the energy increments are minimal for each incremental molecular deformation resulting from changes in the dihedral angle of the driven ring. The resultant route (path B, as in Figure 3) is therefore a function of the particular way in which our computations select the manner of ascent to the transition state.

The calculated activation energy of 14.9 kcal/mol brings TPM comfortably into the range of DNMR study. Although there are no experimental results against which the accuracy of our computation can be gauged, the agreement between the experimental barrier for threshold stereoisomerization in trimesitylmethane<sup>11</sup> and that calculated<sup>10</sup> by the present method offers grounds for confidence in the calculated value.

**Tetra-*o*-tolylsilane.** A comprehensive study of TTS involves the six diastereomeric conformers depicted in part I (Figure 5). Because of the lower symmetry of these structures, as compared to TPM, each ring can be driven in two distinct directions, in which  $|\phi|$  initially either decreases or increases; furthermore, some of the conformers have rings which are themselves distinct (i.e., not related by a symmetry operation to any other rings) and therefore can be driven in several ways, with potentially different resultant isomerizations. For example, the (*xxnx*) conformer of  $C_1$  ( $\psi$ -

$S_4$ ) symmetry has four symmetry-differentiated rings, and therefore can be driven in eight different ways. A total of 32 distinct computations thus results for the six conformers. We have investigated the effect of ring driving to initially lower  $|\phi|$  in all 16 possible cases and examined the remaining 16 cases at a more cursory level.

The results of these calculations (using method II<sup>1</sup>) are recorded in Table II. Each series of calculations is given an (arbitrary) alphabetic label. The isomerization corresponding to that label is given next, the descriptors referring to the conformers of Figure 5, part I. The index of the ring which is driven is recorded in the third column, again with reference to the indexing in Figure 5, part I, along with the direction of rotation of the ring. The isomerization which is observed can be described permutationally (see below) and it is convenient to classify each isomerization by the label of the particular set, or *mode*, of permutations to which it belongs,<sup>12,13</sup> as in the fourth column. The activation energy ( $E_a$ ) of the isomerization is given in the fifth column, while the sixth column lists the strain energy of the transition state with reference to a ground state zero for the (xxxx) conformer (Figure 5, part I). The vertical arrangement corresponds to a given isomerization (e.g., series A) grouped with its reverse (series E). Degenerate isomerizations (topomerizations), i.e., series J and V, or isomerizations for which the calculations yield no reverse (because a lower energy alternative exists), i.e., series T and B, appear as separate entries. Isomerizations starting from the same conformer, and which follow identical pathways<sup>14a</sup> despite the fact that different rings are being driven, are also grouped together (i.e., F with D and L, and I with H and Q).

Several of the isomerizations have common features, so that it is only necessary to go through one of these in detail. We have chosen series A for this purpose. Figure 6 records the general pathway followed by this isomerization. As ring 1 is driven counterclockwise,<sup>14b</sup> rings 3 and 4 rotate slightly clockwise, to somewhat less open orientations, until the driven ring becomes closed ( $\phi = 0^\circ$ ), when ring 4 reverses its direction of torsion. As 1 is driven further, 3 and 4 rotate synchronously (arrows, Figure 6). As the transition state is passed, at which time  $\phi$  for ring 1 is  $+20^\circ$ , and full relaxation is permitted, each of 3 and 4 rotate even more to give a structure roughly approximating that in the lower right of Figure 6. Reorientation of the final structure reveals a new arrangement of  $\psi$ - $S_4$  symmetry, with the (nnnx) conformation. This overall pathway is identical with the central part of the isomerization found for TPM (Figure 3), involving the  $\psi$ - $S_4 \rightarrow \psi$ - $S_4$  change.

Based on idealized structures,<sup>15</sup> the resultant isomerization of Fig 6 involves torsions of  $-60, 0, +60, -60^\circ$  for the four aryl groups 1 through 4 consecutively.<sup>14b</sup> Of significance is the fact that of all possible mechanisms, *this is the least motion pathway*, as will readily be seen by inspection of Table II of the accompanying paper,<sup>13</sup> in which a representative set of physical torsions is given for each of the 24 modes which are found in this system. Such inspection reveals that the idealized physical motions consistent with all modes other than mode 10 and (trivially) modes 13 and 15 involve torsional changes whose sum is greater than the  $180^\circ$  in mode 10 and in the pathway found by the present calculations.

An ORTEP stereoview of the transition state for this isomerization is given in Figure 7, viewed down the original  $S_4$  axis of the starting (xxxx) conformer. Molecular parameters of this and all other transition states are recorded in Table III.

The reverse of the series A isomerization, series E, corresponds to the clockwise<sup>14b</sup> driving of ring 4 in the (nnnx) conformer given as product in Figure 6.<sup>16</sup> The structure of

Table II. Results of Ring Driving Computations of the Mechanism of Stereoisomerization of Tetra-*o*-tolylsilane Conformers

Series	Isomerization <sup>a</sup>	Ring driven <sup>b</sup>	Mode <sup>c</sup>	$E_a^d$	$E_T^e$
A	(xxxx) $\rightarrow$ (nnnx)	1-	10	18.8	18.8
E	(nnnx) $\rightarrow$ (xxxx)	2-	10	9.6	17.0
D	(xnnn) $\rightarrow$ (nxxn)	1-	10	10.2	18.7
F <sup>f</sup>	(xnnn) $\rightarrow$ (nxxn) not (nnxx)	3+	10	12.7	21.1
L	(xnxx) $\rightarrow$ (nnxx)	1-	10	12.7	19.6
G	(xnnn) $\rightarrow$ (xnnx)	4+	10	10.4	18.9
M	(xnxx) $\rightarrow$ (nnxx)	3+	10	14.3	21.2
H	(xxnn) $\rightarrow$ (nxxx)	1-	10	11.9	16.6
I <sup>f</sup>	(xxnn) $\rightarrow$ (nxxx) not (nnxx)	3+	10	12.5	17.2
Q	(xxnx) $\rightarrow$ (nnxx)	2-	10	14.8	18.3
R	(xxnx) $\rightarrow$ (nnnn)	4+	10	16.2	19.6
U	(nnnn) $\rightarrow$ (xxxx)	1+	10	4.2	19.3
K	(xnxx) $\rightarrow$ (xxxx)	2-	10	12.4	19.3
S	(xxnx) $\rightarrow$ (xnxx)	3+	10	16.5	19.9
N	(xnxx) $\rightarrow$ (nxxx)	4+	10	10.1	17.0
O	(xxnx) $\rightarrow$ (nnxx)	1-	10	14.7	18.2
T	(nnnn) $\rightarrow$ (nnxx)	1-	7b	1.1	16.3
C	(xnnn) $\rightarrow$ (nxxx)	1+	14	1.8	10.2
P	(xxnx) $\rightarrow$ (nnxx)	1+	14	8.3	11.7
J	(xnxx) $\rightarrow$ (nnxx)	2+	14	5.3	12.2
V <sup>g</sup>	(xxnn) $\rightarrow$ (nnxx)		14	4.4	9.0
B	(xxxx) $\rightarrow$ (xxxx)	1+	3a	20.4	20.4

<sup>a</sup> Conformer designations refer to Figure 5, part I. <sup>b</sup> Refers to the starting conformer, indexed as in Figure 5, part I. Clockwise rotation of the driven ring as viewed toward the center of the molecule is indicated by +, counterclockwise by -. For example, in series A ring 1 is driven in a counterclockwise direction. <sup>c</sup> Refer to ref 13. <sup>d</sup> Activation energy of the isomerization. <sup>e</sup> Strain energy of the transition state for the isomerization (kcal/mol), with reference to the ground state (xxxx) conformer. <sup>f</sup> See text for clarification. <sup>g</sup> Calculated by method I of part I, assuming a transition state of  $\psi$ - $^oD_{2d}$  symmetry.

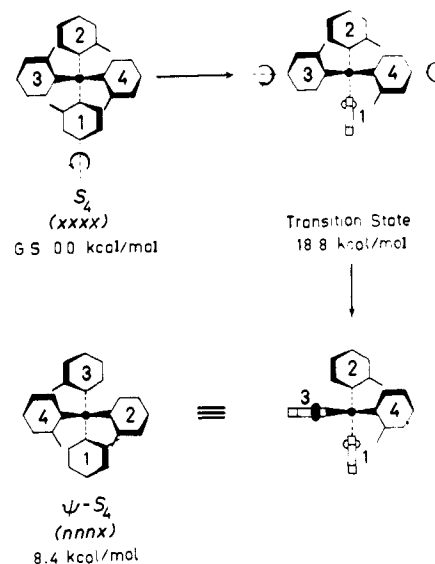


Figure 6. The mechanism of isomerization of (xxxx) tetra-*o*-tolylsilane belonging to mode 10. The ring indexed 1 was driven counterclockwise in increments and all other groups allowed free relaxation.

the transition state is comparable with that given in series A, as is to be expected.<sup>14a</sup> Likewise, the strain energies of the transition states of the two series are similar.<sup>14a</sup>

Table III. Structural Parameters of Transition States of Tetra-*o*-tolylsilane Isomerizations<sup>a</sup>

		A	E	D	L	F	G	M	H	Q	I	K	S
$\phi$	1	19.6	9.5	-6.7	3.2	-30.4	10.0	9.4	-4.1	8.1	-30.2	13.6	16.1
	2	-77.4	-69.4	-66.4	-51.1	-42.3	-71.1	-51.1	-66.3	-64.7	-48.9	-65.6	-59.2
	3	30.2	16.6	38.9	24.3	6.2	39.6	22.9	31.4	18.8	0.3	27.5	20.2
	4	71.9	71.9	61.6	46.4	69.2	53.2	47.6	73.5	63.0	69.1	51.2	47.7
$\theta$	12	116.4	112.6	110.6	113.1	105.2	108.0	112.5	112.0	114.3	105.4	110.1	111.6
	34	107.5	112.3	101.4	105.5	109.9	104.7	112.6	102.7	105.6	106.5	105.4	108.3
	13	105.3	101.5	112.6	104.5	110.4	107.3	102.2	111.3	103.8	114.2	111.7	107.9
	14	111.4	116.9	111.6	108.6	114.3	114.4	109.1	113.5	112.7	114.2	115.2	115.5
	23	106.4	104.9	108.2	109.2	113.4	108.1	105.2	106.4	106.4	109.7	103.1	102.8
	24	109.3	107.6	112.1	115.1	103.5	114.0	114.6	110.4	113.0	106.5	110.6	109.9
$r$	1	1.917	1.901	1.916	1.908	1.918	1.919	1.914	1.917	1.902	1.913	1.913	1.905
	2	1.894	1.887	1.880	1.882	1.875	1.892	1.898	1.870	1.873	1.871	1.906	1.906
	3	1.890	1.885	1.878	1.886	1.903	1.882	1.879	1.883	1.885	1.909	1.883	1.885
	4	1.905	1.916	1.904	1.919	1.916	1.905	1.910	1.903	1.918	1.909	1.910	1.915

<sup>a</sup>The parameters of the first members of each group (i.e., series A, D, G, etc.) are arranged as follows. The numbering for  $\phi$  and  $r$  follows from Figure 6 for the isomerizations belonging to mode 10 (Table II); i.e.,  $\phi_1$  and  $r_1$  refer to the driven ring. The pairs of numbers under  $\theta$  refer to the indices of the two aryl rings subtending the valence angle at the central silicon atom. They are further subdivided into the two originally symmetry differentiated sets, for  $S_4$  or  $\psi$ - $S_4$  symmetry. The parameters of subsequent members of the groupings (i.e., series E, L, F,

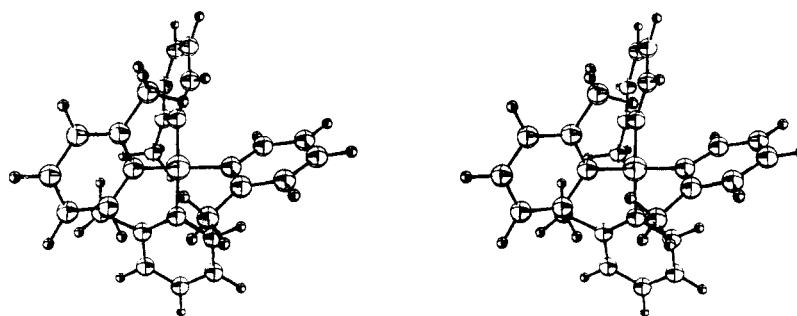


Figure 7. An ORTEP stereopair of the transition state of (xxxx) tetra-*o*-tolylsilane undergoing isomerization by a mechanism belonging to mode 10, observed down the original  $S_4$  axis.

Investigation of the other conformers of TTS reveals a remarkably consistent pattern of isomerization; Figure 6 would suffice to illustrate, in an idealized sense,<sup>15</sup> all the other isomerizations which have been labeled as belonging to mode 10 in Table II, if the relevant positional redistribution of the four methyl substituents were allowed for. In other words, they all follow the same least motion pathway. Again, we note from the tables that the energies and structures of the transition states are similar for pairs of forward-backward isomerizations,<sup>14a</sup> and indeed cover a remarkably narrow range (ca. 17–21 kcal/mol) across the entire series of diastereomeric isomerizations. It will also be noted from Table II that some pairs of isomerizations are apparently duplicated. For instance, both the pairs of series D and L, and G and M effect isomerizations between the (nnnx) and (xnxx) conformers. These overall isomerizations follow the same mechanism (Figure 6) but are distinctly different in that the transition states and pathways are diastereomeric. This particular observation will be useful later when we attempt to construct a route for the overall isomerization of (xxxx) TTS and TNS.

If the mode 10 isomerization is fully general in the TTS system it should be possible to find 16 isomerizations of this type. In fact 16 are found, but only 14 are distinct, F being found equivalent to D, and I to H. The isomerization to be expected for series F, (nnnx)  $\rightarrow$  (nxxx), and its potential inverse, series I, do not take the expected path because of a unique combination of nonbonded interactions in the two starting conformers in question, (nnnx) and (nxxx), respectively. The ring which is driven in each of these two series drives in turn a neighboring ring (one related by a  $\psi$ - $S_4$  op-

eration) by virtue of the closely interacting methyl groups, so that the overall isomerization corresponds to the one which is to be expected if this latter ring were the one to be driven directly. The effect is to duplicate two series, so that F is equivalent to D, and I is identical with H, in overall isomerization consequences. The energies of these pairs of isomerizations are comparable (Table II),<sup>14a</sup> although the transition state parameters appear to differ markedly (Table III). As a consequence of this internal cogwheeling effect, the energetics of the isomerization belonging to mode 10 connecting the (nnnx) and (nxxx) conformers must remain unknown; this method of potential surface investigation is suitable only for finding the lowest energy pathways and cannot be extended to higher energy processes by varying the same internal coordinates.

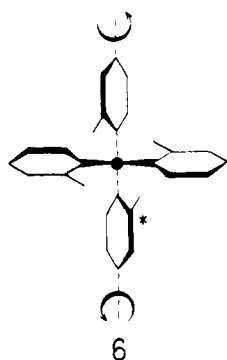
Although the isomerization found in series U is of the same type as the others (mode 10), its derivation differs markedly from those already discussed. The driven ring is *opened* ( $|\phi|$  initially increases), rather than being closed, but as a result of favorable torsions of two other rings, the resultant isomerization belongs to mode 10. The (nnnn) conformer, which is the starting structure for this particular series, differs substantially from the other five diastereomeric conformers, particularly with regard to the low  $|\phi|$  values and the opened valence angles at the silicon atom between the pairs of *o*-tolyl groups related by a  $C_2$  rotation, as already noted in part I. Consequently, particular motions are facilitated: as ring 1 in the (nnnn) conformer opens, ring 3 rotates clockwise, and 4 counterclockwise.<sup>14b</sup> The new structure appears roughly as a (xxxxn) conformation, and indeed collapses to this minimum energy form when the

N	O	R	U	T	C	P	J	V	B
8.7	6.1	19.3	6.7	13.6	88.3	80.6	86.4	89.9	17.6
-64.7	-57.3	-76.6	87.2	-11.1	-73.2	87.4	70.8	90.0	69.4
40.1	29.5	40.1	53.7	12.9	87.5	85.8	-69.0	90.0	-49.7
52.7	55.1	62.4	55.9	21.7	84.2	-73.9	-75.5	90.0	-49.8
109.9	110.4	115.6	110.4	122.5	99.7	97.5	101.8	101.7	100.6
104.2	111.1	105.2	104.8	118.5	98.1	100.2	98.7	101.9	99.9
106.1	102.8	108.4	111.5	103.5	120.0	113.9	116.8	109.0	113.8
114.6	111.9	108.4	108.0	104.6	109.4	114.9	116.9	118.1	120.6
105.1	105.2	107.3	103.5	101.3	116.9	121.9	113.4	118.1	105.6
115.8	114.6	111.5	118.4	107.4	113.3	108.5	109.7	108.9	115.9
1.916	1.908	1.915	1.906	1.907	1.889	1.886	1.882	1.889	1.907
1.894	1.889	1.901	1.902	1.908	1.885	1.890	1.895	1.889	1.891
1.886	1.881	1.882	1.875	1.889	1.883	1.891	1.890	1.890	1.884
1.902	1.911	1.911	1.906	1.885	1.885	1.881	1.882	1.890	1.907

etc.) have been reordered so that they are in a 1:1 correspondence with the first member of the group. Hence,  $\phi$ , and  $r$ , do not refer to the driven ring, and the values of  $\theta$  are no longer arranged with reference to the starting  $S_4$  or  $\psi$ - $S_4$  conformer. Additionally, the signs of  $\phi$  have been normalized across the series to render them mutually comparable, and compatible with Figure 6 in the case of isomerizations belonging to mode 10.

constraints are removed and full relaxation is permitted.

If an aryl ring in the (*nnnn*) conformer is driven to initially lower  $|\phi|$  (i.e., that direction which in all other cases leads to isomerizations belonging to mode 10) as in series T, a totally different isomerization occurs. As the ring marked by an asterisk in **6** is driven through  $-30^\circ$  (arrow)<sup>14b</sup> the



energy increases somewhat but the other groups remain essentially stationary, until the ring related to the driven ring by a  $C_2$  rotation itself rotates  $-30^\circ$  (arrow). The resultant structure has close to  $\psi$ - $D_{2d}$  symmetry and collapses to the (*xnxx*) conformer on full minimization. This mechanism belongs to mode 7b,<sup>13</sup> and is a unique example of this type. Again, this anomaly can be traced to the ground state structure of the (*nnnn*) conformer; since the central valence angle is already enlarged (to  $114.5^\circ$ )<sup>1</sup> the torsions described in **6** are particularly facile. In all other conformers, this mode is prohibited by the relatively greater proximity of the ortho substituents on  $C_2$ -related rings. The (*nnnn*) conformer is stable only by the amount required to effect this isomerization, 1.1 kcal/mol.

The remaining possibilities for computation of dynamic behavior by method II all involve driving one ring to initially higher  $|\phi|$ . We have already discussed the result for the (*nnnn*) conformer. There is a remainder of 15 possible ways in which to accomplish this in the other five conformers, but we have deliberately limited our study of these owing to the predictability of the results. In general, the overall isomerization in each case corresponds to a rocking motion (mode 14) (Figure 8). Hence, we find diastereomerization between the (*nnxx*) and (*xnxx*) conformers in series C and P, and

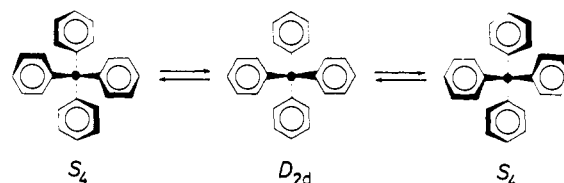


Figure 8. The rocking mechanism, consistent with mode 14, shown for tetraphenylmethane.

topomerizations of the (*xnxx*) and (*xnxx*) conformers in series J and V, respectively. Each was derived as the result of a single ring drive experiment, but it is clear that had any other ring in any of these conformers been chosen, the result would have been the same. All these isomerizations pass through a transition state of roughly  $\psi$ - $D_{2d}$  symmetry (Table III).

However, there is an exception to this trend, in that the expected (*xxxx*)  $\rightleftharpoons$  (*nnnn*) diastereomerization is not observed. As already discussed, the (*nnnn*) conformer as substrate leads to an isomerization belonging to mode 10. Contrary to the expectation that series B would yield the isomerization (*xxxx*)  $\rightarrow$  (*nnnn*), ring driving through  $120^\circ$  yielded the (*xnxx*) conformer (an isomerization belonging to mode 3a). The overall effect is that of a rocking motion (mode 14) followed by an isomerization from mode 10, and series B is best viewed as a composite of these two types. At a stage during the isomerization when it might be expected that the structure would fall into the (*nnnn*) minimum, only a flat region on the hypersurface was encountered. Release of constraints at this stage merely allowed relaxation to the starting (*xxxx*) conformer.<sup>17</sup> The reverse of this isomerization might have been expected in series R. However, in this case the starting (*xnxx*) conformer did lead to the (*nnnn*) conformer, by a mechanism belonging to mode 10, instead of continuing to the (*xxxx*) conformer. The energies of the transition states from series R and B are similar (19.6 and 20.4 kcal/mol, respectively), and so it is not surprising, given the lack of precision inherent in the technique,<sup>14a</sup> that alternative pathways are followed for the two reactions. The reverse of the other exceptional isomerization, series T (mode 7b), was not found in the expected series V because of preferential lower energy topomerization (by ca. 7 kcal/mol).

An implication is that the strain energy of the transition state of the (*xxxx*)  $\rightleftharpoons$  (*nnnn*) isomerization is at least 20.4

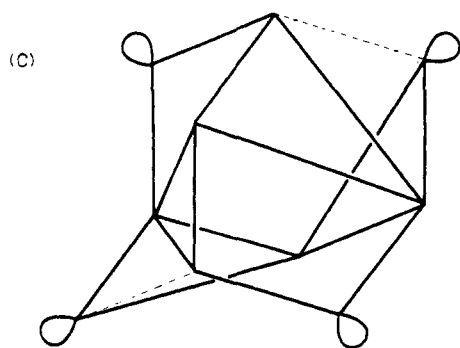
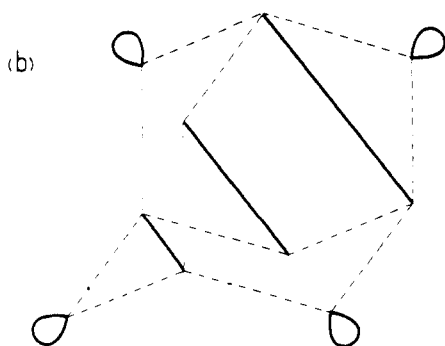
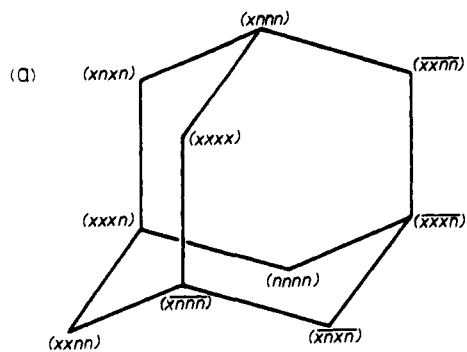


Figure 9. Graphs of tetra-*o*-tolylsilane isomerizations:<sup>19</sup> (a) isomerizations belonging to mode 10; (b) isomerizations belonging to mode 14 (rocking motion); (c) computed isomerizations. Isomer designations are as in part I; enantiomers are distinguished by a bar.

kcal/mol above the ground state, and hence in the TTS system the rocking motion is not always the lowest energy mechanism for isomerization. In other words, there is no unique threshold mechanism. It would therefore be incorrect to analyze the dynamic stereochemistry of this species in terms of the time-average (effective)  $D_{2d}$  point group, as is possible in some other species.<sup>13</sup>

We now turn our attention to convenient pictorial representations of the results we have discussed above. The ten conformers (six diastereomers) of TTS can be represented as vertices of a graph<sup>19</sup> and the isomerizations as edges connecting the relevant vertices (isomers), as in Figure 9. Figure 9a depicts the idealized graph of the isomerizations belonging to mode 10, and Figure 9b the idealized graph of the rocking isomerizations (mode 14). The former is fully connected, so that if all possible isomerizations belonging to mode 10 were able to occur on a given time scale, all conformers of TTS would be equilibrated. In contrast, the

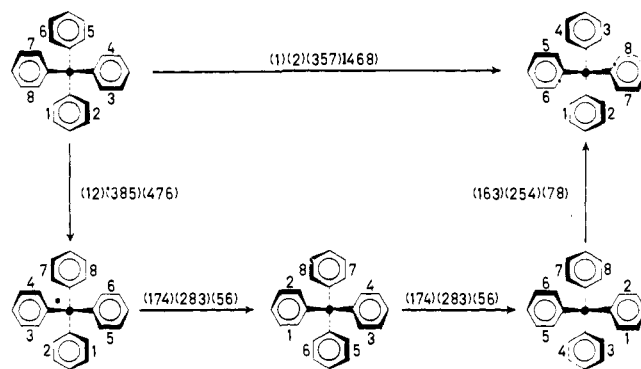


Figure 10. A sequence of four mode 10 permutations equivalent to the single permutation (top arrow) which corresponds to the topomerization of tetra-*o*-tolylsilane.

rocking motion leaves some sets of conformers unconnected, as is intuitively obvious, so that if all possible rocking motions were to occur, but in the absence of all other possible isomerizations, there would be four residual diastereomeric forms<sup>8b</sup> possible for TTS. In Figure 9c is depicted a graph exhibiting all the computed isomerizations. Clearly, the graph is fully connected, and since the highest activation energy to be overcome for any isomerization is ca. 20 kcal/mol, no conformer could be expected to preserve its identity at ambient temperatures. We have already shown in part I that the energy of the ground state (xxxx) conformer is sufficiently low to guarantee it an essentially unique existence, but it is now also clear that none of the other conformers will have any appreciable existence as a metastable form, unless such a state of affairs is imposed upon the species by external conditions, e.g., crystal packing forces. At any rate, the conditions reported for the preparation and isolation of other "stable" conformers of TTS<sup>3</sup> are far in excess of those required to effect conformational changes as evidenced by our computations, and so we can finally lay to rest the possibility that TTS is capable of existing in stable conformationally isomeric forms, as previously claimed.<sup>3</sup>

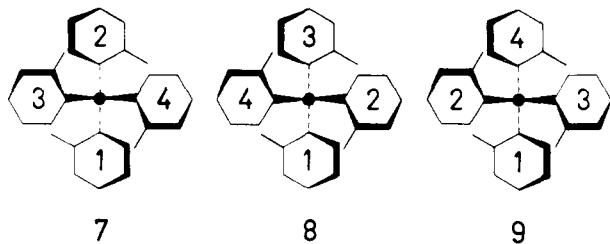
We now turn our attention to how this body of data can serve to explain the DNMR result for TNS which we have previously discussed only on an intuitive level.<sup>4</sup> Before attempting to address this question, however, it will be of benefit to consider the permutational nature of these isomerizations. The accompanying paper<sup>13</sup> gives a thorough treatment of the permutational analysis of the Ar<sub>4</sub>Z system, and we are now in a position to use that analysis to clarify our understanding of the computational results.

The isomerization depicted in Figure 6 is equivalent to that shown vertically on the left in Figure 10, the mode 10 permutation<sup>20</sup> (12)(385)(476) being consistent with the overall physical motions of Figure 6. The two diagrams are easily compared if it is recognized that the odd indices on the structures in Figure 10 can be equated to methyl groups. The period of this permutation is six.<sup>21</sup> Accordingly, if TTS isomerizes solely by a mechanism belonging to mode 10, six barriers are encountered in the course of a full rotation about a single *o*-tolyl-silicon bond by  $2\pi$  radians:<sup>22</sup> (xxxx)  $\rightarrow$  (nxxx)  $\rightarrow$  (xnxx)  $\rightarrow$  (nxxx)  $\rightarrow$  (xnxx)  $\rightarrow$  (nxxx)  $\rightarrow$  (xxxx). The initial and final conformations have the same pairings of *o*-tolyl groups, and this is therefore not a pathway which would effect an isomerization consistent with the DNMR results<sup>2</sup> of TNS.

Using the accompanying analysis<sup>13</sup> it can be deduced that the permutations of mode 10 suffice to generate the complete feasible group for tetraarylmethane stereoisomerization,  $G_{192} \cong A_4[S_2]$ . Hence, since the mechanism corresponding to mode 10 is so prevalent, the following impor-

tant result can be stated: *there will be no residual diastereomers in a maximally labeled (and consequently any submaximally labeled) tetraarylmethane.* This applies whether any rocking motions are occurring or not.

We are now in a position to follow through with an investigation of the isomerization of TTS and TNS. The question to be answered is: what are feasible sequences of isomerization steps which will effect the interconversion of the conformers 7, 8, and 9?



of the structures with the identity permutation (1)(2)(3)(4)(5)(6)(7)(8) (i.e., the reference structure<sup>20</sup> in Figure 10), then the other two are related to the former by the permutations (1)(2)(375)(486) and (1)(2)(357)(468) respectively.<sup>23</sup> The question then reduces to what sequence of mode 10 permutations, with or without mode 14 (rocking) permutations, generate either of these two permutations, or their six equivalents<sup>23</sup> from the identity (see Figure 10). Once this question is answered, the problem of the TNS DNMR behavior becomes trivial since it is easy to imagine one of the *o*-tolyl groups in each of 7, 8, and 9 being replaced by a 1-naphthyl group.

Our approach to this problem has been to resort to a computer program<sup>24</sup> which accepts for input any number of permutations and multiplies them together to exhaustion, ensuring group closure. The mode 10 permutations were used as input, and since it is possible to keep track of the derivation of each new permutation as it is generated, a sequence of mode 10 permutations which give a required product permutation can be derived. Since the product permutations are even and the mode 10 permutations are odd, it immediately follows that there must be an even number of the latter to effect isomerization, if isomerization occurs only by a path corresponding to that mode. The shortest sequence found by this method contains no less than four permutations and is depicted in Figure 10. It is now an easy matter to "translate" the permutations back into appropriate physical motions. The corresponding pathway is shown in Figure 11, with relevant energies of intermediates and transition states indicated. Note that the second and third steps are *not* the reverse of each other, although they involve the conformer sequence (nnnx)  $\rightarrow$  (nxnx)  $\rightarrow$  (nnnx). As discussed earlier, the two isomerizations in question are diastereomeric and are taken one from each of the two pairs of series D and L, and G and M (Table II).

There is no reason to exclude permutations corresponding to the rocking motion in the isomerization scheme. Since these permutations are even, they must be combined with an even number of mode 10 permutations. As previously, sequences of four permutations were computed which led to a desired product permutation. Each of these contained two mode 14 permutations, one of which was either the first or last in the sequence. The latter possibility is not as likely since it would involve a rocking motion not found during the ring driving experiments, and whose activation energy is predicted to be greater than 20.4 kcal/mol. The former possibility would in actuality involve the mechanism belonging to mode 3a as first step, since again no pure rocking motion leading from the (xxxx) TTS conformer to the (nnnn) con-

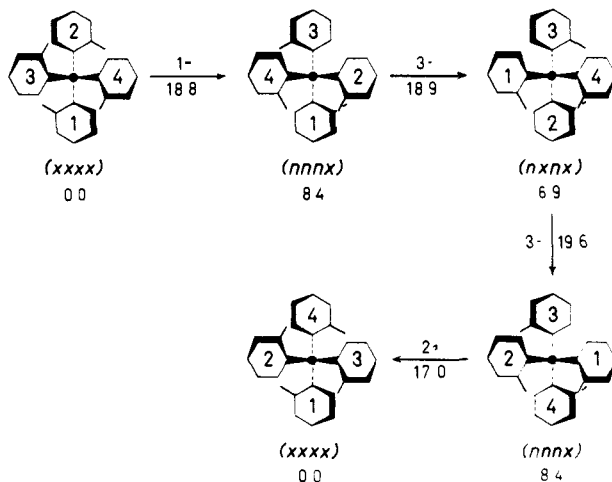


**Figure 11.** A pathway for the topomerization of tetra-*o*-tolylsilane by four consecutive isomerizations belonging to mode 10. Strain energies of intermediates and transition states are given in kcal/mol. The index of the driven ring is given above each arrow, with its direction of torsion according to the convention that positive = clockwise as viewed toward the center of the molecule.<sup>14b</sup>

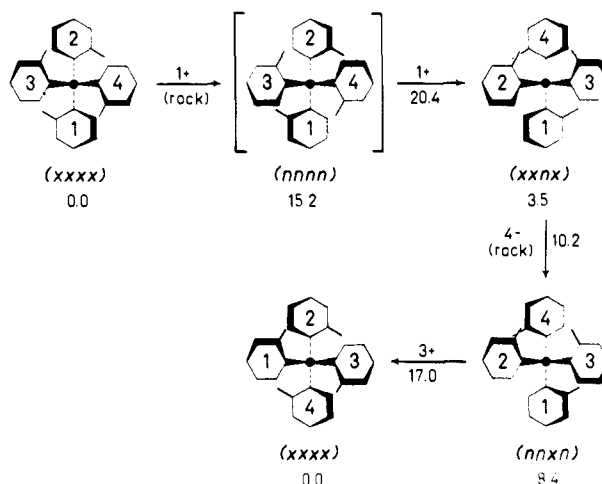


**Figure 12.** A pathway for the topomerization of tetra-*o*-tolylsilane by a combination of isomerizations belonging to modes 10 and 14. See caption of Figure 11 and text for clarification.

former was computed. This fact is emphasized in Figure 12 in which the four isomerizations formally corresponding to the computed permutations are depicted in full, but where the potential (nnnn) intermediate is enclosed in brackets to signify that the structure is bypassed in actuality. The overall isomerization in this case would therefore involve only three steps and two intermediates. This pathway is the one with the least number of isomerization steps. However, we note that in principle there are an infinite number of routes involving all the mechanisms recorded in Table II, all involving a greater number of isomerization steps. Therefore, employing Occam's Razor, we opt for the pathways depicted in Figures 11 and 12.

To effect site exchange of the three methyl groups in TNS, a further topomerization sequence is necessary. For instance, repetition of the pathway outlined in Figure 11 (i.e., a total of eight distinct isomerizations) starting from the product isomer depicted therein would give that isomer containing the remaining possible pairings of aryl groups (i.e., 1 with 3 and 2 with 4). All *o*-tolyl groups would hence be rendered equivalent, as required by the observed DNMR results.<sup>2</sup>



These computed mechanisms may be compared with the two-step pathway derived intuitively and reported in an earlier paper.<sup>4</sup> The first stage of that pathway is, in fact, an isomerization belonging to mode 10. However, the second part of the pathway follows a mechanism we have not observed in our computations, belonging to mode 11*b*.

The activation energy measured by DNMR techniques for the stereoisomerization of TNS is 13.5 kcal/mol,<sup>2</sup> and since all evidence from the comparable triaryl systems<sup>25</sup> points to the fact that an *o*-methyl substituent is only slightly more sterically encumbered than benzo, we felt justified in setting an upper limit of 16 kcal/mol for the isomerization of TTS.<sup>2</sup> In the schemes given above (Figures 11 and 12), the computed activation energies are 19.6 and 20.4 kcal/mol, respectively. The agreement between the experimentally derived and computed values is already quite satisfactory, but we believe that the computational results are, in fact, even closer to the observed value, for two reasons. First, it has proven possible in favorable circumstances to unlock all constrained atoms of the structure at the computed transition state and allow further *full relaxation* energy minimization without the transition state structure collapsing to either the starting or the final structures. This results from the transition state occurring at a particularly flat region of the potential hypersurface, so that group torsions are not particularly favored. Consequently, the strain energy of the transition state is further optimized but without departing from the desired geometry. In series D, the energy fell at least 3 kcal/mol without changing the overall geometry of the constrained transition state, which suggests that all our calculations may have overestimated the transition state energy by approximately this amount, since the same constraints were implicit in all of them. The second line of evidence derives from a ring driving experiment on tris(2,6-xylyl)silane, in precisely the same manner as reported for the series B calculations on trimesitylmethane.<sup>10</sup> Whereas in the all-carbon system the computed value<sup>10</sup> was slightly less than the experimentally determined value,<sup>11</sup> by about 2 kcal/mol, the calculation on the silane yielded a value 2.1 kcal/mol *in excess* of the experimentally determined 10.9 kcal/mol.<sup>26</sup> Hence, either the constraints inherent in the computations, or features of the parametrization of the force field which are dependent on silicon, cause the strain energies of the transition states of arylsilanes to be overestimated. Making an empirical correction of 3 kcal/mol for all the values in Table II therefore brings our computed values for the activation energy of the isomerization of TTS into gratifying agreement with the barrier estimated on the basis of the DNMR experiments with TNS.<sup>2</sup>

**Acknowledgment.** We gratefully acknowledge support of this research by the National Science Foundation (MPS74-18161). M.G.H. wishes to thank the Salters' Company for the award of a Fellowship (1972-1974).

## References and Notes

- M. G. Hutchings, J. D. Andose, and K. Mislow, *J. Am. Chem. Soc.*, preceding paper in this issue.
- M. G. Hutchings, C. A. Maryanoff, and K. Mislow, *J. Am. Chem. Soc.*, **95**, 7158 (1973).
- G. N. R. Smart, H. Gilman, and H. W. Otto, *J. Am. Chem. Soc.*, **77**, 5193 (1955).
- M. G. Hutchings, J. G. Nourse, and K. Mislow, *Tetrahedron*, **30**, 1535 (1974).
- (a) D. E. Fenton, A. G. Massey, K. W. Jolley, and L. H. Sutcliffe, *Chem. Commun.*, 1097 (1967); (b) K. W. Jolley and L. H. Sutcliffe, *Spectrochim. Acta, Part A*, **24**, 1191 (1968).
- In part I it was noted that TTS may possess a further minimum energy conformation of  $D_2$  symmetry, which is, however, of relatively minor importance.
- R. S. Cahn, C. Ingold, and V. Prelog, *Angew. Chem., Int. Ed. Engl.*, **5**, 385 (1966).
- (a) C. M. Woodman, *Mol. Phys.*, **19**, 753 (1970); L. Radom and J. A. Pople, *J. Am. Chem. Soc.*, **92**, 4786 (1970); (b) P. Finocchiaro, D. Gust, and K. Mislow, *ibid.*, **96**, 3198, 3205 (1974).
- R. Stolevik, *Acta Chem. Scand., Ser. A*, **28**, 327 (1974).
- J. D. Andose and K. Mislow, *J. Am. Chem. Soc.*, **96**, 2168 (1974).
- P. Finocchiaro, D. Gust, and K. Mislow, *J. Am. Chem. Soc.*, **96**, 2165 (1974).
- The numbering of modes in the present paper corresponds precisely to that employed in the accompanying paper,<sup>13</sup> which should also be consulted for further details. It is emphasized that the permutational representation implies nothing about the physical motions inherent in a particular mechanism. However, the rigorous statement that the permutational consequences of a particular isomerization are represented by a permutation in mode 10 has been abbreviated throughout this paper by the statement that the isomerization belongs to mode 10.
- J. G. Nourse and K. Mislow, *J. Am. Chem. Soc.*, following paper in this issue.
- (a) In principle, the values of  $E_T$  for an isomerization and its reverse should be identical, as should the geometries of the transition states. The differences which are in fact observed are due to the constraints which are inherent both in the method used (see part I) and in the minimization module,<sup>10</sup> being reflected unequally in the forward and backward isomerizations. For the same reason, the results for series F differ from D, and I from H, although the pairs of isomerizations are mutually equivalent. A similar effect was noted from the two series of analogous calculations on trimesitylmethane, which differed by 0.7 kcal/mol.<sup>10</sup> (b) In the following discussion, the convention is adopted that positive and negative directions of rotation refer to clockwise and counterclockwise motions, respectively, as viewed toward the center of the molecule.
- We assume  $\phi = \pm 60^\circ$  for the idealized  $S_4$  and  $\psi$ - $S_4$  structures given in the figures. Hence, any isomerization results from a combination of torsions which are integral multiples of  $60^\circ$ .
- It should be noted that the indexing of the rings in Figure 6 and subsequent figures may unavoidably fail to correspond to that of Figure 5, part I, and Table II, which are in turn mutually compatible. For example, while the indexing of the rings in the (xxxx) conformer is the same in Figures 7 and 5, part I, the indexing of the rings in the (nnn) isomer is not.
- This computation also included the only example we have found of a false minimum. The energy decreased prior to the transition state, but release of constraints led back to the starting isomer. This observation is not unexpected and is a function, and drawback, of this particular computational method.<sup>18</sup>
- J. W. McIver, Jr., and A. Komornicki, *J. Am. Chem. Soc.*, **94**, 2625 (1972).
- The frame on which we have chosen to construct the graphs is isostructural with the adamantane molecule. The broken lines in these graphs are only given to assist visualization and do not correspond to isomerizations; they are a ghost of the image upon which the graphs proper are delineated.
- The conformation in the top left of Figure 10 is defined as the reference structure, where the numbers shown refer both to site and ligand indices.<sup>4,13</sup> For details of how the permutations act on the site indices, see ref 4 and 13.
- In contrast, the rocking motion is described by a mode 14 permutation of period 2, such as (14)(23)(58)(67).
- The second step in the sequence does not correspond to any of the computed isomerizations (Table II); rather, it is the result of the idealized series F isomerization, which belongs to mode 10. As discussed in the text, the actual result of the series F computation is the (nxxn) conformer. The driven ring changes helicity in the course of this isomerization, so that if ring driving is continued in the same direction, a new mechanism, rocking, occurs. This is in turn followed by an infinite loop connecting the (xnnn) and (xxxn) conformers (i.e., series K and O). Hence, continuous driving of a ring in the (xxxx) conformer, following least energy pathways throughout, will never regenerate the (xxxx) conformer.
- There are six other equally acceptable permutations, equivalent to these two by double transpositions of aryl groups, two of which correspond to  $C_2$  rotations, and the other four of which involve change of helicity<sup>4,13</sup> without altering ring pairings.
- The program was written in these laboratories by Gilbert J. Chin.
- J. F. Blount, P. Finocchiaro, D. Gust, and K. Mislow, *J. Am. Chem. Soc.*, **95**, 7019 (1973).
- R. J. Boettcher, D. Gust, and K. Mislow, *J. Am. Chem. Soc.*, **95**, 7157 (1973).